

# Study on Controllable Preparation of Silica Nanoparticles with Multi-sizes and Their Size-dependent Cytotoxicity in Pheochromocytoma Cells and Human Embryonic Kidney Cells

Huihui Yuan,<sup>a, b, c</sup> Feng Gao,<sup>d</sup> Zhigang Zhang,<sup>a</sup> Ledo Miao,<sup>a</sup> Ronghua Yu,<sup>a</sup>  
Hongli Zhao,<sup>a, b</sup> and Minbo Lan<sup>\*, a, b</sup>

<sup>a</sup>Shanghai Key Laboratory of Functional Materials Chemistry, and Research Center of Analysis and Test, <sup>b</sup>Key Laboratory for Ultrafine Materials of Ministry of Education, <sup>c</sup>The Institute of Applied Chemistry and <sup>d</sup>Department of Pharmaceutics, School of Pharmacy, East China University of Science and Technology, 130 Meilong Road, Shanghai, 200237, P.R. China

(Received March 18, 2010; Accepted August 12, 2010)

High-tech products made by nano-materials are tightly connected to people's life. However environmental impacts and health effects of nanoparticles are widely getting attention. In this paper, we focused on the potential size-dependent cytotoxicity of nanomaterials. Silica (SiO<sub>2</sub>) nanoparticles were used as model material. The ion exchange method and modified StÖber method were used to controllably prepare monodisperse uniform silica nanoparticles with six types of size (20, 50, 80, 140, 280 and 760 nm). And the 3-(4,5-dimethylthiazol-2-yl)-2,5-diphenyltetrazolium bromide (MTT) assay and cellular morphology were introduced to evaluate the effect of the six sizes SiO<sub>2</sub> nanoparticles on pheochromocytoma (PC12) and human embryonic kidney (HEK293) cells viability. The results indicated that nanosized-SiO<sub>2</sub> (20, 50 and 80 nm) caused more cell damage when compared with microsized-SiO<sub>2</sub> (140, 280 and 800 nm). IC<sub>50</sub> of 24 hr exposure in PC12 cells were 118.2 ± 7.3, 320.4 ± 9.8, and 380.7 ± 10.5 µg/ml, and in HEK293 cells were 80.2 ± 6.4, 140.3 ± 9.6 and 309.2 ± 11.3 µg/ml for 20, 50- and 80-nm SiO<sub>2</sub> particles, respectively. Additionally, the SiO<sub>2</sub> particles of the other three sizes over 80-nm had little influence on the cell viability at the concentrations below 2000 µg/ml for two cultured cells. The results suggested that the exposure of SiO<sub>2</sub> nanoparticles with different sizes led to cellular morphological modifications and apoptosis in a size-dependent manner. Further studies on the molecular mechanisms of apoptosis and the toxicity *in vivo* are necessary.

**Key words** — silica nanoparticle, controllable preparation, cytotoxicity, size-dependent

## INTRODUCTION

Nanotechnology has enabled significant advances in the areas of electronic information,<sup>1)</sup> medicine,<sup>2,3)</sup> cosmetic,<sup>4)</sup> and new energy fields.<sup>5)</sup> While in 2006, there were more than 300 commercial products available on the market that were claimed to have enhanced properties due to the incorporated nanomaterials, this number has more than doubled in 2008.<sup>6)</sup> The increasing production

has led to calls for more information regarding the potential impacts that releases of these materials may have on human and environmental health.<sup>7)</sup>

More and more researchers began to pay attention to the safety issue of the nanomaterials,<sup>8,9)</sup> but the overwhelming majorities of such studies are related to the risk of nanomaterials themselves. The harm resulted from nanomaterials with different sizes were seldom reported. Only the cytotoxicity induced by nano and fine-sized particles were investigated and compared.<sup>10,11)</sup> In this case, the detailed mechanism leading to nanoparticles cytotoxicity is not yet fully understood. It is necessary to make a systemic evaluation on cytotoxicity of nanomaterials in different size. Silica (SiO<sub>2</sub>) nanoparticles with good stability, chemical inertia, biocompatible

\*To whom correspondence should be addressed: Research Center of Analysis and Test, East China University of Science and Technology, 130 Meilong Road, Shanghai, 200237, P.R. China. Tel.: +86-21-64253574; Fax: +86-21-64252947; E-mail: minbolan@ecust.edu.cn

property and single spherical form, have been widely used in dope, rubber, plastic, and others which are vitally related to people's life. Nozawa and Serdobintseva have succeeded in the preparation of monodisperse  $\text{SiO}_2$  particles with sizes above 100 nm.<sup>12,13</sup> However, the preparation of controllable monodisperse uniform  $\text{SiO}_2$  particles with desired size less than 100 nm was difficult. But, the nucleation and growth mechanisms of  $\text{SiO}_2$  made it possible by using ion-exchange method with optimized preparation process.<sup>14</sup> So, monodisperse uniform  $\text{SiO}_2$  nanoparticles could be one of the most representative and compatible materials used as model to investigate the safety of nanomaterials in size.

The purpose of this study attempted to investigate the size-impact of monodisperse uniform nanoparticles on pheochromocytoma (PC12) cells and human embryonic kidney (HEK293) cells. And  $\text{SiO}_2$  nanoparticles with six sizes (20, 50, 80, 140, 280 and 760 nm) used in this evaluation system should be comprehensive and persuasive. So, we focused on using ion exchange method to controllably prepare monodisperse uniform  $\text{SiO}_2$  nanoparticles with size less than 100 nm and introducing modified StÖber method to prepare the  $\text{SiO}_2$  nanoparticles with sizes 140, 280 and 760 nm respectively.<sup>12</sup> Then, the nanoparticle-induced cytotoxicities on PC12 cells and HEK293 cells were studied.

## MATERIALS AND METHODS

**Materials**—Sodium silicate and sodium hydroxide were brought from Chinese Curative Shanghai Chemical Reagent Company (Shanghai, China). Cation resin (732) was supplied by Shanghai Huazhen Technology and Trade Company (East China University of Science and Technology, Shanghai, China). Ammonia, dimethyl sulfoxide (DMSO) and ethyl silicate were brought from Shanghai Lingfeng Chemical Reagent Limited Company (Shanghai, China). Anhydrous ethanol was brought from Shanghai Shengde Chemistry Limited Company (Shanghai, China). Dulbecco's modified Eagle's medium (DMEM), penicillin, streptomycin, horse serum and fetal bovine serum (FBS) were purchased from Invitrogen (Carlsbad, CA, U.S.A.). MTT, Triton X-100, propidium iodide, bovine serum albumin and tetraethoxypropane were purchased from Sigma Chemical Company (St. Louis, MO, U.S.A.). All reagents were of ana-

lytical grade. All aqueous solutions were prepared in deionized water.

**Preparation of Amorphous  $\text{SiO}_2$  Nanoparticles**—The preparation of amorphous  $\text{SiO}_2$  nanoparticles with sizes less than 100 nm was as follows:  $\text{SiO}_2$  nanoparticles were prepared by a modified ion exchange method.<sup>14</sup> Briefly, diluted aqueous sodium silicate solution was passed through a bed of cation resin and an aqueous solution of active silica acid was obtained. This solution was comprised of about 2% suspending  $\text{SiO}_2$  particles with a diameter of 2 nm or less and its pH was of 1.5–2.5. The active silica acid was added into sodium hydroxide solution with pH of 10–12 by peristaltic pump (BT00-50 M, Glanze, Baoding, China) under refluxing and the reaction pH value was greater than 9.<sup>14</sup> When the reaction came to completion (1–2 hr after the addition of active silica acid), the resulting sol A was used as the seed sol for a further growth reaction leading to a second generation of silica sol B, and then the desired amounts of active silica acid was added into B under different addition rate to give sols C and D, respectively. The reaction was kept for another 1–2 hr to ensure that the particles could reach their final size. The process was repeated until there were monodisperse nanoparticles in the new sol, according to details given in Table 1. And amorphous  $\text{SiO}_2$  nanoparticles with sizes more than 100 nm were controllably prepared by the modified StÖber method.<sup>12</sup>

**Analysis of Silica Sol and Nanoparticles**—The pH value of silica sol were measured by precise pH meter (PHS-2S, DDS-11A, Dapu instruments limited company, Shanghai, China). The morphology of  $\text{SiO}_2$  nanoparticle was measured by transmission electron microscope (TEM-1200EXII, JEOL, Tokyo, Japan), scanning electron microscope (SEM, Philips XL30, Philips, Eindhoven, Holland), respectively. The size distribution and mean size of nanoparticles were determined on a dynamic light scattering (DLS), ZETASIZER-3000HS (Malvern Instruments, Malvern, UK).

**Cell Culture**—The undifferentiated PC12 cell line and the HEK293 cell line were purchased from cell bank of Chinese Academy of Sciences (Shanghai, China). PC12 cells were cultured in a full DMEM medium containing 10% inactivated horse serum, 5% FBS, 100 U/ml penicillin and 100  $\mu\text{g}/\text{ml}$  streptomycin, and incubated at 37°C in a humidified atmosphere containing 5%  $\text{CO}_2$ . HEK293 cells were cultured in a full DMEM medium containing 10% FBS, 100 U/ml penicillin and 100  $\mu\text{g}/\text{ml}$  strep-

**Table 1.** Experimental Conditions Used for Preparation of SiO<sub>2</sub> Nanoparticles

Sample	Initial sol <sup>a)</sup>	Active silicic acid		
		Addition rate <sup>b)</sup>	Volume (ml)	pH
A-1	100 ml water	1.5	100	1.91
B-1-a	30 ml A-1	2.0	60	1.88
B-1-b	30 ml A-1	1.0	60	1.94
B-1-c	30 ml A-1	1.5	60	1.97
B-1-d	30 ml A-1	1.5	60	2.12
B-1-e	30 ml A-1	5.0	60	2.09
A-2	50 ml water	1.7	50	2.42
B-2	30 ml A-2	1.7	30	2.43
C-2-a	30 ml B-2	1.7	30	2.32
C-2-b	30 ml B-2	1.7	40	2.40
C-2-c	20 ml B-2	1.7	30	2.22

a) All of the initial sols were diluted to 60 ml. Water was used as initial sol in preparation of sample A-1 and B-2. b) Addition rate was the value of peristaltic pump, and the actually rate was  $y$  (ml/min) from equation:  $y = 0.1825x + 0.0161$   $R^2 = 0.9997$  in which  $x$  is the value in this table.

tomycin, and incubated at 37°C in a humidified atmosphere containing 5% CO<sub>2</sub>.

**SiO<sub>2</sub> Nanoparticles Exposure** — The stock sols of SiO<sub>2</sub> nanoparticles with certain size were sterile filtered and stored at 4°C. In each study, the stock sols were freshly diluted to different concentrations in the cell culture medium. For the MTT assay, PC12 cells and HEK293 cells were plated into a 96-well plate at a density of  $1.0 \times 10^4$  cells per well in 100  $\mu$ l culture medium. After cells had attached for 12 hr in the full medium, the medium was replaced with low serum DMEM (containing 0.1% FBS) to prevent nanoparticle agglomeration. Freshly dispersed particle sols were immediately applied to the cells. Cells free of SiO<sub>2</sub> nanoparticles were used as control cells throughout each assay.

**Assessment of Cytotoxicity** — Cell viability was measured by the MTT assay.<sup>15)</sup> Following the treatment, the cells were incubated with MTT (0.5 mg/ml) for 4 hr. The medium was then removed and 100  $\mu$ l of DMSO were added into each well to dissolve formazan crystals, the metabolite of MTT. After thoroughly mixing, the plate was read at 570 nm for optical density that is directly correlated with cell quantity. Cell viability was calculated from the relative absorbance at 570 nm and expressed as the percentage of control. Dose-dependency of cellular toxicity was plotted from MTT results.

**Qualitative Observation of Cellular Morphology** — Cells were plated into a 24-well plate at a density of  $1.0 \times 10^5$  cells per well. Following cells were exposed as mentioned above at various concentrations of SiO<sub>2</sub> nanoparticles for 24 hr, HEK293

cells were washed in ice-cold phosphate buffered saline (PBS) and fixed with 10% paraformaldehyde and then stained with haematoxylin and eosin to improve visualization and observed under an XSP-17C inverted phase contrast microscope (Changfang Optical Instruments, Shanghai, China). PC12 cells were observed by an XSP-17C microscope directly after completion of the exposure period.

**Flow Cytometric Analysis of Cellular Apoptosis** — HEK293 cells (or PC12 cells) were seeded in a six-well culture plate at a density of  $2.0 \times 10^5$  cell/well. After the SiO<sub>2</sub> treatments, the cells were collected, fixed and permeabilized with 75% ice-cold ethanol overnight at 4°C. The cells were then washed with PBS and resuspended in 1 ml of lysis buffer [0.1% Triton X-100, 0.05 mg/ml propidium iodide, and 1 mg/ml ribonuclease (RNase A)]. After 30 min incubation at 37°C, the cells were analyzed in a FACScan flow cytometer (Becton Dickinson, Franklin Lakes, NJ, U.S.A.) at 488 nm excitation and 620 nm emission. The percentage of cellular apoptosis was calculated by standard ModiFit and CellQuest software programs.

## RESULTS AND DISCUSSION

### Particle Growth via Seeded Experiments

In order to produce monodisperse SiO<sub>2</sub> nanoparticles of various desired sizes, the optimal experiment conditions, such as pH value of the system, rate of addition and concentration of the initial sol, were selected as shown in Table 1. And

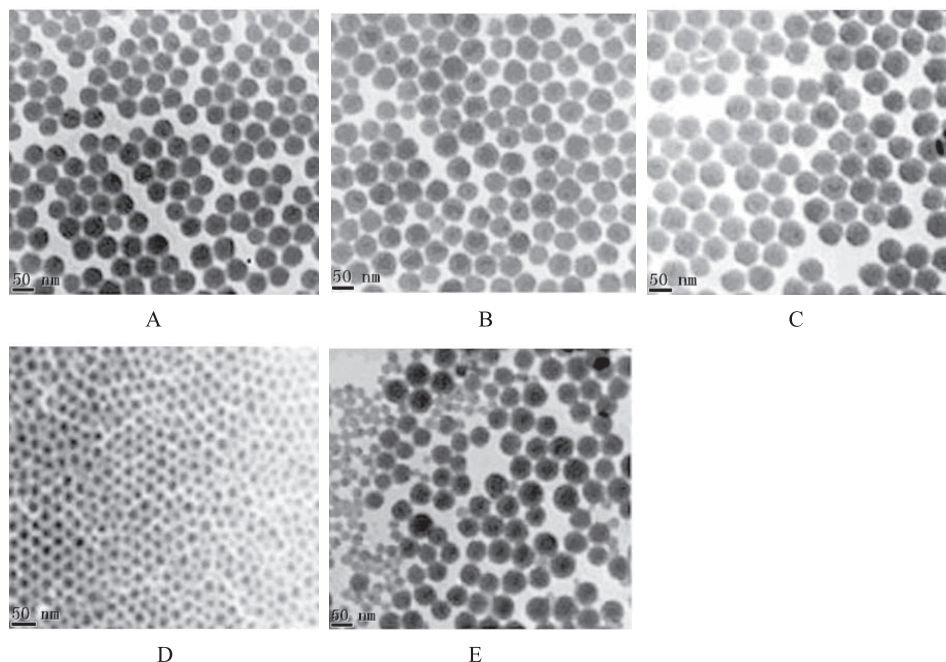


**Fig. 1.** TEM Images of SiO<sub>2</sub> Nanoparticles

SiO<sub>2</sub> nanoparticles were prepared by different conditions showed in Table 1. Samples were (A) B-1-a, (B) B-1-b, (C) B-1-c, (D) B-1-d, and (E) B-1-e.

**Table 2.** Size Analysis of SiO<sub>2</sub> Nanoparticles by DLS Measurement

Sample	Z mean (nm)	Intensity mean (nm)	Volume mean (nm)	Polydispersity
C-2-a	33.9	34.7	30.6	0.04
C-2-b	45.8	45.0	43.7	0.10
C-2-c	66.7	63.2	57.7	0.25

a series of nanoparticles was obtained from sol of sample A-1 (Fig. 1) under the different reaction conditions.

The silicic acid underwent dehydration and condensation polymerization to form nuclei firstly by heating in the presence of alkali, then deposited around the nuclei, and thus particles were formed. In fact, nucleation and particle growth took place simultaneously. In Fig. 1D showed the TEM image of sample B-1-d prepared by the method mentioned above without controlling the pH value. A lot of new nuclei were found around the grown particles, which meant nucleation and particle growth took place simultaneously. Therefore, pH control was considered to be one of the most important factors for preparing monodisperse uniform SiO<sub>2</sub> nanoparticles.

Figure 1A–1C and 1E showed SiO<sub>2</sub> nanoparticles of Sample B-1-a, b, c and e, which were resulted from different addition rates of active silicic acid of 0.20, 0.27, 0.38 and 0.87 ml/min, respectively. Little difference was among Fig. 1A–1C, and all nanoparticles were almost monodisperse, uni-

form and spherical without new nuclei. Figure 1E showed so many new nuclei among the grown SiO<sub>2</sub> nanoparticles for fast addition rate. Quantitatively, it was found that an addition rate of 0.1–0.3 ml/min of active silicic acid would avoid the renucleation due to the high local concentration.

Table 2 listed the mean diameters and polydispersity of sample C-2-a, b and c. And their experimental conditions were showed in Table 1. The results presented the influences of the seed sol concentration and the volume of the addition active silicic acid on the final particle size distribution. The decrease in concentration of the seed sol or the increase in the volume of active silicic acid would enlarge the final particle sizes under the same reactive condition. Moreover, the polydispersity was becoming larger with the increase of particle mean size.

Thus, the above experimental parameters should be smartly controlled to prepare uniform SiO<sub>2</sub> nanoparticles with small polydispersity and constant nuclei.

**Table 3.** The Results of SiO<sub>2</sub> Nanoparticles in Smart Controllable Experiments

Sample	Experimental conditions		SiO <sub>2</sub> nanoparticles		$W_f/W_i + 1$	$(D_f/D_i)^3$
	Initial sol <sup>a)</sup>	Volume <sup>b)</sup> (ml)	Z mean (nm)	Polydispersity		
A-3	60 ml water	60	30.3	0.13	—	—
B-3	20 ml A-3	40	45.4	0.08	—	—
C-3-a	20 ml B-3	40	73.5	0.03	4.20	4.24
C-3-b	20 ml B-3	57	80.6	0.03	5.56	5.60
C-3-c	15 ml B-3	20	62.8	0.04	3.13	2.65
C-3-d	15 ml B-3	4	51.8	0.08	1.43	1.48

a) All of the initial sols were diluted two times except the sample A-3. Water was used as initial sol in preparation of sample A-3. b) Addition volume of active silicic acid.

### Smart Size Control of Monodisperse SiO<sub>2</sub> Nanoparticles

Monodisperse uniform SiO<sub>2</sub> nanoparticles could be achieved through controllable nucleation and growth of particles in dilute sol. Furthermore, smart size control of monodisperse uniform SiO<sub>2</sub> nanoparticles could be established in selecting the optimal experimental parameters in our research system by adjusting the volume of active silica acid. It is hypothesized that active silica acid added only increases the particle size, but not forms new nuclei. And the total number of particles in the system would remain constant. As a result, the mass density of SiO<sub>2</sub> remained constant in the system which could be mathematically showed as:

$$\rho = W_t / (N \times 6\pi D_i^3) = (W_t + W_0) / (N \times 6\pi D_f^3) \quad (1)$$

Where  $W_t$  was the weight of active SiO<sub>2</sub> added to the seed sol and  $W_0$  was the weight of SiO<sub>2</sub> initially present as nuclei, respectively.  $\rho$  was the mass density of SiO<sub>2</sub>;  $N$  was the total number of particle; and the particle diameter would increase from the initial size  $D_i$  to the final size  $D_f$ . When  $W_t/W_0$  was defined as build-up ratio  $Br$ , equation (1) could be adjusted as<sup>16)</sup>

$$(D_f/D_i)^3 = Br + 1. \quad (2)$$

Equation (2) was used to illuminate the controllability of particle growth in many reports.<sup>17, 18)</sup>

In our study, smart control of particle size was carried out by varying the active silicic acid volume added to the seed sol, with the other experimental parameters fixed. Table 3 showed the impact of different active silicic acid volume on the particle growth progress, with the rest of conditions identical: the concentration of seed sol B-3 with 6.0 mg/ml, agitation rate of 800 rpm, addition rate of 0.17 ml/min, reactive time and refluxing. The results of sample C presented a good tendency that the

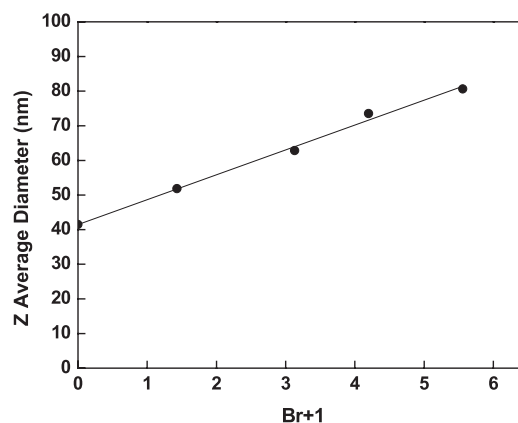


**Fig. 2.** Relationship between Z Average Diameter of SiO<sub>2</sub> Nanoparticle and  $Br + 1$

Where  $Br + 1: (D_f/D_i)^3$ .

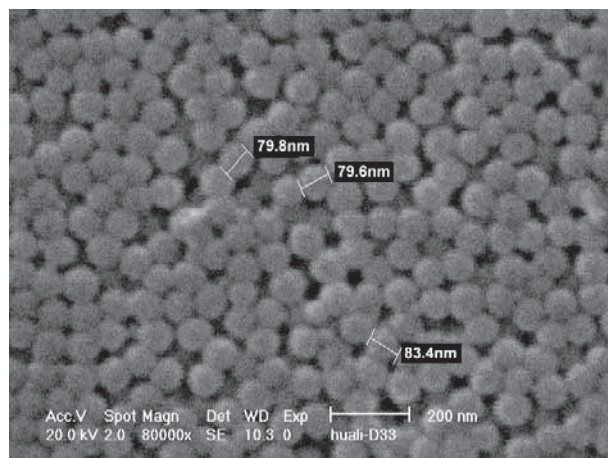


**Fig. 3.** SEM Images of 80-nm SiO<sub>2</sub> Particles

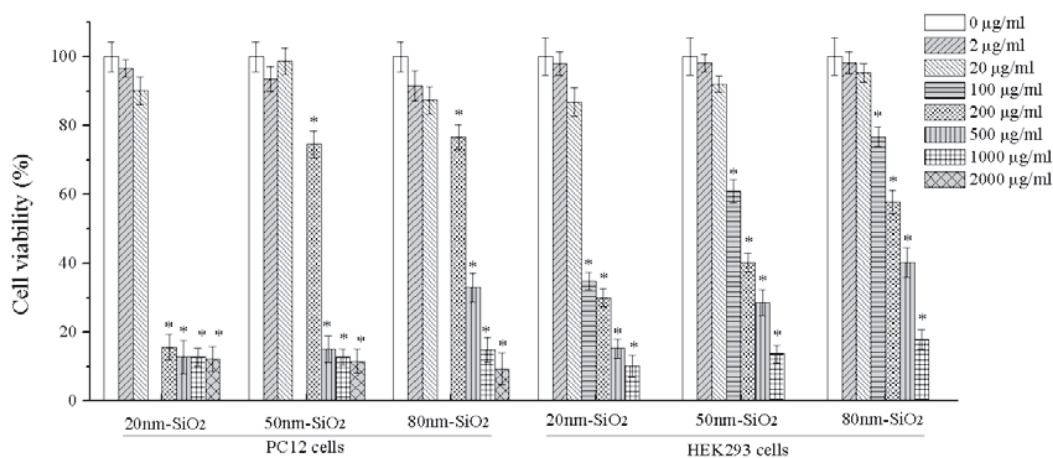
final particle size increased from 51.8 to 80.6 nm while the value of polydispersity decreased from 0.08 to 0.03. The smaller value of polydispersity indicated the better monodispersity of particle.

Figure 2 showed a good linear relationship between final size and  $Br + 1$ . The fitted equation was  $D_f = 41.48 + 7.1774(Br + 1)$  ( $r = 0.9942$ ). And Fig. 3 showed the image of the nanoparticles

**Table 4.** Effect of SiO<sub>2</sub> Nanoparticles with Six Sizes on PC12 and HEK293 Cells Viability

Desired size (nm)	Z mean (nm)	Polydispersity	IC <sub>50</sub> (μg/ml)	
			PC12 cells	HEK293 cells
20	21.2	0.04	118.2 ± 7.3	80.2 ± 6.4
50	48.6	0.03	320.4 ± 9.8	140.3 ± 9.6
80	80.1	0.06	380.7 ± 10.5	309.2 ± 11.3
140	143.2	0.05	> 2000	> 2000
280	281.0	0.01	> 2000	> 2000
760	763.0	0.03	> 2000	> 2000

Values of IC<sub>50</sub> were the mean ± S.D. from three independent experiments.

**Fig. 4.** Dose-dependent Toxicity of Different Sizes of Nano-SiO<sub>2</sub> in PC12 Cells and HEK293 Cells

with the designed size of 80 nm formed by adding calculated volume of active silica acid to a sol of preformed nuclei. It also appeared to be highly monodisperse with a polydispersity less than 0.08. In addition, by such a build-up operation, particles of any desired diameter under 100 nm could be prepared through two or three growing steps as long as there were no tendency towards particle agglomeration and renucleation.

Consequently, the simplicity of this method opened new prospects in controllable synthesis of uniform SiO<sub>2</sub> nanoparticles with desired size. And it was possible for safety assessments of nanoparticles with different sizes less than 100 nm *in vitro* and *in vivo*. The parameters of desired size prepared by above method and optimal conditions were shown in Table 4.

#### Cytotoxicity of SiO<sub>2</sub> Nanoparticles with Six Sizes

PC12 cells and HEK293 cells were exposed to SiO<sub>2</sub> nanoparticles with six sizes at the concentrations from 20 to 2000 μg/ml for 24 hr, respectively.

It was found in Fig. 4 that cell viability decreased as the particle sizes diminished and dosage levels augmented. The viability of cells exposed to the three sizes nano-SiO<sub>2</sub> particles decreased significantly at concentrations above 20 μg/ml compared with that of control. The IC<sub>50</sub> values of SiO<sub>2</sub> nanoparticles with different sizes were calculated and presented in Table 4. It was obvious that the IC<sub>50</sub> values increased with the particle size. The results of the two cells assess showed the common tendency that the 20-nm SiO<sub>2</sub> particles had more remarkable cytotoxicity than 50-nm SiO<sub>2</sub> particles. The 80-nm SiO<sub>2</sub> particles had unobvious cytotoxicity. And the SiO<sub>2</sub> particles of the other three sizes over 80 nm had little influence on the cell viability at the concentrations below 2000 μg/ml for PC12 cells and HEK293 cells.

#### Effect of SiO<sub>2</sub> Nanoparticles on Cellular Morphology and Apoptosis

SiO<sub>2</sub> nanoparticle-induced cytotoxicity in PC12 cells and HEK293 cells was further confirmed. Their morphological changes of cells were exam-

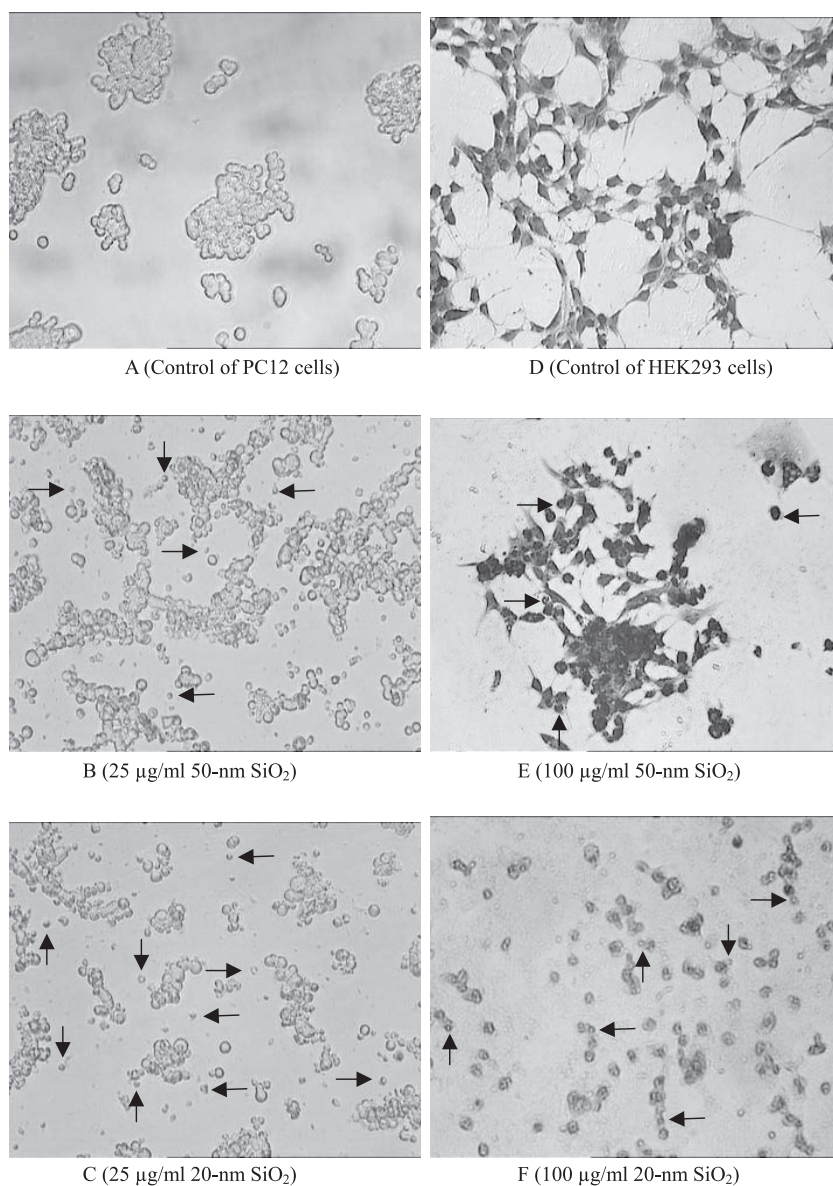


**Fig. 5.** Morphological Characterization of PC12 Cells and HEK293 Cells

Cells were exposed to 20- and 50-nm SiO<sub>2</sub> particles for 24 hr, and visualized under a microscope (magnification 100×). PC12 cells (in A, B and C); HEK293 cells (in D, E and F).

ined using inverted phase contrast microscope. The control PC12 cells were round in shape with numerous cells conjuncted (Fig. 5A). Figure 5B and 5C showed that PC12 cells treated with SiO<sub>2</sub> nanoparticle were much smaller and many of them were fragmented as indicated by the arrows. The conjunction of cells was broken more remarkably when cells were exposed to the 20-nm SiO<sub>2</sub> particles (Fig. 5C). Figure 4D showed the morphology of control HEK293 cells. Similarly, the cells presented the features of apoptosis such as cell shrinkage, irregular shapes, and nuclear condensation (arrows indicated in Fig. 5E and 5F), and the interconnec-

tion of cells was badly destroyed when cells were treated with SiO<sub>2</sub> nanoparticles, especially with 20-nm SiO<sub>2</sub> particles (Fig. 5F). Thus, the 20-nm SiO<sub>2</sub> particles seemed to be more cytotoxic than the 50-nm SiO<sub>2</sub> particles. Size-dependent cytotoxic effects were well demonstrated (Fig. 5). The same trend of cellular apoptosis was presented in Table 5. Both PC12 cells and HEK293 cells treated with 20-nm SiO<sub>2</sub> particles had higher apoptosis percentage than with 50-nm SiO<sub>2</sub> particles.

In conclusion, the ion exchange method with optimal experimental parameters could be used to controllably prepare the uniform SiO<sub>2</sub> nanoparti-

**Table 5.** The Apoptosis Proportion of Cells after Exposure to Nano-SiO<sub>2</sub>

SiO <sub>2</sub> (nm)	Dosage (µg/ml)	Apoptosis (% of cells)	
		PC12 cells	HEK293 cells
control	0	0.5 ± 0.4	0.6 ± 0.9
20	50	6.8 ± 1.8*	11.2 ± 2.6*
20	100	15.9 ± 3.1*	34.4 ± 7.9*
50	50	4.5 ± 1.6*	8.9 ± 2.1*
50	100	14.5 ± 7.9*	29.6 ± 5.7*

The cells were exposed to SiO<sub>2</sub> nanoparticles for 24 hr, then cells were harvested and analyzed for cell cycle and apoptosis using flow cytometry. Values were mean ± S.D. from three independent experiments. \**p* < 0.05 versus control.

cles at desired size with good monodispersity. And SiO<sub>2</sub> particles at 20, 50 and 80 nm were prepared and the desired sizes successfully agreed with the calculated sizes by the fitted equation. In addition, SiO<sub>2</sub> particles with diameters of 140, 280 and 760 nm were obtained by the modified StÖber method. SiO<sub>2</sub> nanoparticles with six sizes were monodispersed, which polydispersity were all below 0.06. In the present study, the cytotoxicity of six sizes of SiO<sub>2</sub> nanoparticles was investigated in cultured neuronal cells and human embryonic kidney cells. Sharma<sup>19)</sup> had reported the effects of chronic silicon dioxide nanoparticles (40–50 nm) exposure on spinal cord injury induced alterations on the functional outcome and the cord pathology in a rat model, and indicated that exposure of nanoparticles enhanced the sensitivity of central nervous system to injuries and altered the effect of neuroprotective drugs. The MTT results indicated that nano-SiO<sub>2</sub> (20, 50 and 80 nm) caused more cell damage when compared with microsized-SiO<sub>2</sub> (140, 280 and 800 nm). Researches on nanoparticle cytotoxicity of oxide metal, organic materials or co-particles gave the same conclusion.<sup>10, 20, 21)</sup> This was probably due to larger specific surface area and micro-pore volume for interaction,<sup>22)</sup> smaller sizes for cell penetration<sup>23, 24)</sup> and from the nanoparticles. Cell morphology study also confirmed that the smaller the particle is, the greater its toxicity is.<sup>25–27)</sup> Although the cytotoxic character of nanoparticles has been reported in numerous investigations involving SiO<sub>2</sub>, TiO<sub>2</sub>, Ni, polyvinylchloride (PVC), iridium, ZnO, fullerene and so on,<sup>28–30)</sup> the cytotoxicity comparison among different nanomaterials was inaccurate due to the polydispersity and size differences of those nanoparticles. Furthermore, it was difficult to explore the detailed mechanism at molecular level. Our preliminary data has suggested that expo-

sure of SiO<sub>2</sub> nanoparticles with different sizes leads to cellular morphological modifications and apoptosis in a size-dependent manner.<sup>24)</sup> Further studies are underway to investigate the molecular mechanisms of apoptosis, as well as the toxicity *in vivo*.

**Acknowledgements** This work was supported by the Science and Technology Commission of Shanghai Municipality (STCSM, No. 10dz2220500).

## REFERENCES

- Hai, A., Dormann, A., Shappir, J., Yitzchaik, S., Bartic, C., Borghs, G., Langedijk, J. P. M. and Spira, M. E. (2009) Spine-shaped gold protrusions improve the adherence and electrical coupling of neurons with the surface of micro-electronic devices. *J. R. Soc. Interface*, **6**, 1153–1165.
- Chun, Y. W. and Webster, T. J. (2009) The Role of Nanomedicine in Growing Tissues. *Ann. Biomed. Eng.*, **37**, 2034–2047.
- Jiang, W., Kim, B. Y. S., Rutka, J. T. and Chan, W. C. W. (2008) Nanoparticle-mediated cellular response is size-dependent. *Nat. Nanotechnol.*, **3**, 145–150.
- Keck, C. M. and Schwabe, K. (2009) Silver-nanolipid complex for application to atopic dermatitis skin: rheological characterization, *in vivo* efficiency and theory of action. *J. Biomed. Nanotechnol.*, **5**, 428–436.
- Chandra, A., Roberts, A. J., Yee, E. L. H. and Slade, R. C. T. (2009) Nanostructured oxides for energy storage applications in batteries and supercapacitors. *Pure Appl. Chem.*, **81**, 1489–1498.
- Ku, B. K., Emery, M. S., Maynard, A. D., Stolzenburg, M. R. and McMurphy, P. H. (2006) In situ structure characterization of airborne carbon nanofibres by a tandem mobility-mass analysis. *Nanotechnology*, **17**, 3613–3621.
- Colvin, V. L. (2003) The potential environmental impact of engineered nanomaterials. *Nat. Biotechnol.*, **21**, 1166–1170.
- Zollanvari, A., Cunningham, M. J., Braga-Neto, U. and Dougherty, E. R. (2009) Analysis and modeling of time-course gene-expression profiles from nanomaterial-exposed primary human epidermal keratinocytes. *Bmc Bioinformatics*, **10**, S10.
- Hoet, P., Legiest, B., Geys, J. and Nemery, B. (2009) Do nanomedicines require novel safety assessments to ensure their safety for long-term human use? *Drug Saf.*, **32**, 625–636.
- Sayes, C. M. and Warheit, D. B. (2008) An *in vitro*



- investigation of the differential cytotoxic responses of human and rat lung epithelial cell lines using TiO<sub>2</sub> nanoparticles. *Int. J. Nanotechnol.*, **5**, 15–29.
- 11) Warheit, D. B., Sayes, C. M. and Reed, K. L. (2009) Nanoscale and fine zinc oxide particles: can in vitro assays accurately forecast lung hazards following inhalation exposures? *Environ. Sci. Technol.*, **43**, 7939–7945.
  - 12) Nozawa, K., Gailhanou, H., Raison, L., Panizza, P., Ushiki, H., Sellier, E., Delville, J. P. and Delville, M. H. (2005) Smart control of monodisperse sto1ber silica particles: effect of reactant addition rate on growth process. *Langmuir*, **21**, 1516–1523.
  - 13) Serdobintseva, V. V., Kalinin, D. V., Danilyuk, A. F., Plehanov, A. I., Kurdyukov, D. A. and Rudina, N. A. (2005) Mechanism of the growth of monodispersed spherical silica particles to the submicron size. *React. Kinet. Catalysis Lett.*, **84**, 389–394.
  - 14) Lan, M. B., Yuan, H. H. and Miao, L. D. (2004) Preparation method of silica nanoparticles used for standard nanoparticles. CN Patent, China, 200410025419.9.
  - 15) Denizot, F. and Lang, R. (1986) Rapid colorimetric assay for cell growth and survival: modifications to the tetrazolium dye procedure giving improved sensitivity and reliability. *J. Immunol. Methods*, **89**, 271–277.
  - 16) Iler, R. K. (1979) *The Chemistry of Silica*, Wiley, New York.
  - 17) Sada, E., Kumazawa, H. and Koresawa, E. (1990) Reaction kinetics and size control in the formation of monosized silica spheres by controlled hydrolysis of tetraethyl orthosilicate in ethanol. *Chem. Eng. J.*, **44**, 133–139.
  - 18) Cheng, S. L., Dong, P., Yang, G. H. and Yang, J. J. (1996) Characteristic aspects of formation of new particles during the growth of monosize silica seeds. *J. Colloid Interface Sci.*, **180**, 237–241.
  - 19) Sharma, H. S., Patnaik, R., Sharma, A., Sjöquist, P.-O. and Lafuente, J. V. (2009) Silicon dioxide nanoparticles (SiO<sub>2</sub>, 40–50 nm) exacerbate pathophysiology of traumatic spinal cord injury and deteriorate functional outcome in the rat. an experimental study using pharmacological and morphological approaches. *J. Nanosci. Nanotechnol.*, **9**, 4970–4980.
  - 20) Midander, M., Cronholm, P., Karlsson, H. L., Elihn, K., Moller, L., Leygraf, C. and Wallinder, I. O. (2009) Surface characteristics, copper release, and toxicity of nano- and micrometer-sized copper and copper(ii) oxide particles: a cross-disciplinary study. *Small*, **5**, 389–399.
  - 21) Valavanidis, A., Fiotakis, K. and Vlachogianni, T. (2008) Airborne particulate matter and human health: toxicological assessment and importance of size and composition of particles for oxidative damage and carcinogenic mechanisms. *J. Environ. Sci. Health C.*, **26**, 339–362.
  - 22) Napierska, D., Thomassen, L. C. J., Rabolli, V., Lison, D., Gonzalez, L., Kirsch-Volders, M., Martens, J. A. and Hoet, P. H. (2009) Size-dependent cytotoxicity of monodisperse silica nanoparticles in human endothelial cells. *Small*, **5**, 846–853.
  - 23) Faraji, A. H. and Wipf, P. (2009) Nanoparticles in cellular drug delivery. *Bioorg. Med. Chem.*, **17**, 2950–2962.
  - 24) Wang, F., Gao, F., Lan, M. B., Yuan, H. H., Huang, Y. P. and Liu, J. W. (2009) Oxidative stress contributes to silica nanoparticle-induced cytotoxicity in human embryonic kidney cells. *Toxicol. In Vitro*, **23**, 808–815.
  - 25) Kipen, H. M. and Laskin, D. L. (2005) Smaller is not always better: nanotechnology yields nanotoxicology. *Am. J. Physiol. Lung Cell. Mol. Physiol.*, **289**, 696–697.
  - 26) Oberdorster, G., Oberdorster, E. and Oberdorster, J. (2005) Nanotoxicology: an emerging discipline evolving from studies of ultrafine particles. *Environ. Health Perspect.*, **113**, 823–839.
  - 27) Nel, A., Xia, T., Madler, L. and Li, N. (2006) Toxic potential of materials at the nanolevel. *Science*, **311**, 622–627.
  - 28) Peters, K., Unger, R. E., Kirkpatrick, C. J., Gatti, A. M. and Monari, E. (2004) Effect of nano-scaled partricles on endothelial cell function in vitro: studies on viability, proliferation and inflammation. *J. Mater. Sci. Mater. Med.*, **15**, 321–325.
  - 29) Sayes, C. M., Marchione, A. A., Reed, K. L. and Warheit, D. B. (2007) Comparative pulmonary toxicity assessments of C-60 water suspensions in rats: few differences in fullerene toxicity in vivo in contrast to in vitro profiles. *Nano Lett.*, **7**, 2399–2406.
  - 30) Semmler, M., Seitz, J., Erbe, F., Mayer, P., Heyder, J., Oberdorster, G. and Kreyling, W. G. (2004) Long-term clearance kinetics of inhaled ultrafine insoluble iridium particles from the rat lung, including transient translocation into secondary organs. *Inhal. Toxicol.*, **16**, 453–459.